RSC Advances

RSC Publishing

PAPER

View Article Online
View Journal | View Issue

Cite this: *RSC Adv.*, 2013, **3**, 20673

The supramolecular structure is decisive for the immunostimulatory properties of synthetic analogues of a mycobacterial lipid *in vitro*†

Birte Martin-Bertelsen,‡[a] Karen Smith Korsholm,‡[b] Fabrice Rose,[a] Pernille Nordly,[ab] Henrik Franzyk,[c] Peter Andersen,[b] Else Marie Agger,[b] Dennis Christensen,[b] Anan Yaghmur[a] and Camilla Foged*[a]

Identification of new vaccine adjuvants with immunopotentiating properties commonly involves *in vitro* evaluations of candidate compounds for their ability to stimulate cells of the immune system. Subsequent elaborate experiments are then performed on only the positive candidates. Here we show how this strategy may miss good candidates due to context-dependent supramolecular characteristics of the candidate compounds, since both a specific molecular structure and the correct presentation of specific parts of the compounds are required for successful stimulation of the cells. Nevertheless, the supramolecular structure is rarely evaluated although changes in this structure may have a drastic impact on the presentation of the compounds to the cells. Synthetic analogues of the mycobacterial cell wall lipid monomycoloyl glycerol (MMG) possess immunopotentiating properties, but their biophysical characteristics are largely unresolved and the structural features determining their immunoactivating properties have been poorly explored. In the present study, we demonstrate that the immunostimulatory activity *in vitro* correlates with the supramolecular characteristics of the self-assembled MMG nanostructures. Thus, a series of MMG analogues displaying different stereochemistry in the hydrophobic moiety and the polar headgroup were designed and synthesized with different alkyl chain lengths. Stimulation of human monocyte-derived dendritic cells *in vitro* was clearly dependent on the stereochemistry of the hydrophobic part and on the alkyl chain length but not on the stereochemistry of the hydrophilic glycerol moiety. Small-angle X-ray scattering (SAXS) analysis showed that the immunoactivating analogues self-assembled into lamellar phases whereas the biologically inert analogues adopted inverse hexagonal phases. Langmuir monolayers confirmed that analogues with opposite lipid acid configurations displayed different packing modes. These data demonstrate that the biophysical properties and the lipid molecular structure are major determinants for the ability of the MMG analogues to activate antigen-presenting cells. Our findings emphasize the importance of investigating the biophysical and structural properties when assessing the effect of adjuvants *in vitro*.

Received 3rd June 2013
Accepted 28th August 2013

DOI: 10.1039/c3ra42737d

www.rsc.org/advances

1 Introduction

Vaccination has been successfully used as an effective means of preventing infectious diseases and reducing disease burden, but efficient vaccines are still not available for certain infectious diseases such as AIDS, malaria and tuberculosis (TB). A promising strategy is the subunit vaccine technology, which is based on well-defined and highly purified antigenic components of the pathogen combined with immunopotentiating compounds that enhance and control the nature of the immune response. These immunopotentiating compounds, termed adjuvants, often resemble pathogen-associated molecular patterns (PAMPs) and they can activate the immune system by interacting with pattern-recognition receptors (PRRs) on antigen-presenting cells (APCs). Adjuvants are thus often initially evaluated and characterized by their ability to stimulate APCs *in vitro*. Examples of adjuvants are monophosphoryl lipid A (MPL), which has been shown to stimulate the cells through binding to Toll-like receptor 4[1] and trehalose dibehenate (TDB) and trehalose dimycolate (TDM), which signal through the C-type lectin receptor (CLR) Mincle.[2,3]

[a]*Department of Pharmacy, Faculty of Health and Medical Sciences, University of Copenhagen, Universitetsparken 2, DK-2100 Copenhagen O, Denmark. E-mail: camilla.foged@sund.ku.dk*

[b]*Department of Infectious Disease Immunology, Vaccine Adjuvant Research, Statens Serum Institut, Artillerivej 5, DK-2300 Copenhagen S, Denmark*

[c]*Department of Drug Design and Pharmacology, Faculty of Health and Medical Sciences, University of Copenhagen, Universitetsparken 2, DK-2100 Copenhagen O, Denmark*

† Electronic supplementary information (ESI) available. See DOI: 10.1039/c3ra42737d

‡ These authors contributed equally.

Both a specific structure and the correct presentation of specific parts of the immunopotentiating compounds are required for the interaction with the PRRs and the subsequent activation of the APCs. However, the biophysical behavior of the self-assembled nanostructures formed by the surfactant-like compounds under the fully hydrated *in vitro* conditions is rarely evaluated, although changes in the structure may influence the presentation of the compounds to the APCs. The reason for this is most likely that the use of advanced biophysical techniques is required for the structural characterization, which in practice necessitates interdisciplinary collaborations.

The lipid monomycoloyl glycerol (MMG) has been identified *in vitro* as the most immunopotentiating compound among a number of different lipids isolated from the mycobacterial cell wall.[4] The natural occurring form of MMG is too toxic for human use but some well-tolerated synthetic analogues have been shown to possess immunopotentiating properties similar to the natural compound.[4] The analogue MMG-1 described by Nordly *et al.* is based on a simple C_{32} lipid acid with a stereochemistry corresponding to an alternative (A) configuration of the corynomycolic acid compared to the natural MMG compound (Fig. 1). The synthetic isomeric analogue MMG-6, which is shown in Fig. 1 as a comparison, is an example of an analogue configuration with a stereochemistry corresponding to the native (N) configuration of the corynomycolic acid. MMG-1 consists of a glycerol headgroup linked *via* an ester bond to a hydrophobic lipid acid displaying two saturated alkyl chains (C_{14} and C_{15}, respectively). Upon incorporation of this neutral, double-tailed, surfactant-like lipid into liposomes based on the quaternary ammonium salt dimethyldioctadecylammonium (DDA) bromide, the otherwise unstable cationic DDA liposomes are stabilized, most likely due to an improved hydration of the MMG-1 headgroups protruding into the lipid–water interfacial space.[5] In addition, DDA/MMG-1 liposomes have been shown to induce a strong cell-mediated immune response characterized by antibody production and mixed T-helper responses with high secretion levels of the effector cytokines interferon γ (IFN-γ) and interleukin 17 (IL-17) in mice. Such characteristics are attractive for the development of vaccines against *e.g.* TB. *In vivo* studies with MMG derivatives also indicate that different structural analogues may possess diverse immunopotentiating properties upon incorporation into the bilayer of cationic liposomes.[6]

In the present study, the effect of systematically varying the headgroup stereochemistry and the length of the hydrophobic alkyl chains of MMG on the immunopotentiating properties was examined by stimulating human monocyte-derived dendritic cells (DCs) *in vitro*. Small-angle X-ray scattering (SAXS) was subsequently used to identify the nanostructures formed under similar fully hydrated conditions, and the biophysical properties of the formed lipid monolayers were evaluated by using the Langmuir technique. These biophysical characteristics were finally correlated to the immunostimulatory activities of the different structural MMG analogues.

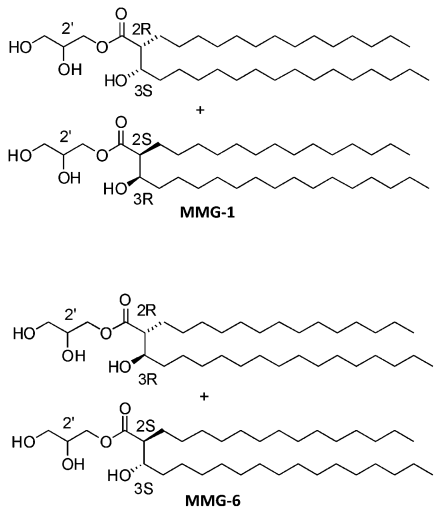

Fig. 1 Comparison of the two possible relative configurations of MMG analogues, exemplified by MMG-1 (alternative configuration) and MMG-6 (native configuration). The alternative compounds display (2*R*,3*S*) and (2*S*,3*R*) configurations in a 1 : 1 ratio in the lipid acid moieties while the native compounds contain lipid acid moieties displaying (2*R*,3*R*) and (2*S*,3*S*) configurations. The depicted alkyl chain length is C_{14}/C_{15}.

2 Materials and methods

Materials

The used chemicals and reagents were obtained commercially at analytical grade.

Synthesis of MMG analogues

Several different MMG analogues with varying stereochemistry and lipid chain lengths were synthesized (Table 1). The analogues were synthesized as described previously.[5] The identity of the resulting compounds was confirmed by NMR (see ESI† data for details of NMR data).

Differentiation of human monocyte-derived DCs

Cryopreserved peripheral blood mononuclear cells (PBMCs) purified from buffy coats from anonymous human blood donors by Ficoll-Hypaque density gradient centrifugation were thawed rapidly at 37 °C in a water bath and washed twice in complete RPMI medium [RPMI 1640 supplemented with 2 mM sodium pyruvate, 1% (v/v) non-essential amino acids, 10 mM HEPES, 100 U mL^{-1} penicillin and 100 μg mL^{-1} streptomycin

Table 1 Overview of the designed MMG analogues[a]

Name	Headgroup stereochemistry	Stereochemistry of lipid acid moieties	Chain lengths
MMG-1 (A)	2′*R*	(2*R*,3*S*)/(2*S*,3*R*)	C_{14}/C_{15}
MMG-2 (A)	2′*R*	(2*R*,3*S*)/(2*S*,3*R*)	C_{16}/C_{17}
MMG-3 (A)	2′*R*	(2*R*,3*S*)/(2*S*,3*R*)	C_{10}/C_{11}
MMG-4 (A)	2′*R*	(2*R*,3*S*)/(2*S*,3*R*)	C_6/C_7
MMG-5 (A)	2′*S*	(2*R*,3*S*)/(2*S*,3*R*)	C_{14}/C_{15}
MMG-6 (N)	2′*R*	(2*R*,3*R*)/(2*S*,3*S*)	C_{14}/C_{15}
MMG-7 (N)	2′*S*	(2*R*,3*R*)/(2*S*,3*S*)	C_{14}/C_{15}

[a] A: alternative racemic corynomycolic acid configuration. N: native racemic corynomycolic acid configuration.

(Invitrogen, Taastrup, Denmark) with 10% (v/v) heat-inactivated fetal bovine serum (FBS superior, standardized, VWR, Leicestershire, England)]. Monocytes were subsequently enriched by negative selection by using the EasySep Human Monocyte Enrichment kit (Stemcell Technologies, Grenoble, France) according to the manufacturer's instructions. After purification, the cells were washed and seeded into tissue culture-treated Nunclon 6-well plates (NUNC) at a density of 2×10^6 cells per well in 4 mL complete RPMI with 10% FBS supplemented with 100 ng mL^{-1} recombinant human IL-4 and 200 ng mL^{-1} recombinant human GM-CSF (granulocyte macrophage-colony stimulating factor) (Peprotech, Stockholm, Sweden). The cells were incubated at 37 °C in a 5% CO_2–95% atmospheric air incubator. After 7 days, the cells had differentiated into immature DCs.

In vitro stimulation of DCs with MMG analogues

For stimulation of DCs, the series of MMG analogues was coated onto tissue culture plates in concentrations ranging from 0.3–219 μg mL^{-1} in 3-fold serial dilutions. The MMG analogues were dissolved in and diluted to the desired concentrations with ultrapure isopropanol (Sigma-Aldrich). An amount of 20 μL per well of the dissolved MMG analogues was transferred into flat-bottomed Nunclon 96-well culture plates (NUNC). The plates were left without lids overnight in a laminar flow bench at room temperature to allow for the complete evaporation of isopropanol. For stimulation, 2×10^5 DCs in 200 μL complete RPMI/FBS were transferred into each well of the lipid-coated plates. As a positive control, 100 ng mL^{-1} LPS was added to the cells in the absence of MMG, and as a negative control, the cells were added to empty or isopropanol-treated wells. The cells were stimulated at 37 °C in a 5% CO_2–95% atmospheric air incubator. The supernatants were harvested after 18–22 h and kept at −20 °C until cytokine analysis. The stimulated cells were immediately transferred into V-bottomed 96-well plates for viability assessment.

Cytokine analysis and assessment of cell viability

The release of interleukin 6 (IL-6), interleukin 8 (IL-8), and tumor necrosis factor α (TNF-α) by the stimulated DCs was assessed by ELISA using the OptEIa human IL-6, IL-8 or TNF-α sets according to the manufacturer's instructions (BD Pharmingen, San Diego, California). Due to the high donor-to-donor variation, the data were normalized according to the maximal response of each individual donor. The cytotoxicity was assessed by staining the cells with the Green Viability dye (GrVid) (Invitrogen/Molecular probes) for 30 min in the dark at 4 °C. The cells were washed and subsequently analyzed by using a FACSCanto flow cytometer (BD Biosciences). The GrVid dye penetrates dead and apoptotic cells and these can thus be visualized in the FITC channel. The fraction of dead cells was calculated as the ratio between $FITC^+$ and $FITC^-$ cells.

Preparation of fully hydrated samples for SAXS analysis

The samples were prepared by using a thin-film method. Briefly, weighed amounts of MMG analogues were dissolved in $CHCl_3$–MeOH (9 : 1, v/v). The solutions were dried under a gentle stream of N_2 for at least 1 h and subsequently evaporated under vacuum resulting in the formation of a thin lipid film. The dry lipid film was hydrated by adding Tris buffer (10 mM, pH 7.4) and carrying out at least five freeze–thaw cycles between liquid nitrogen and room temperature and then homogenizing several times during the thawing steps by vigorous vortexing and heating at 60 °C. The final lipid concentration was 100 mg mL^{-1} and the samples were incubated at room temperature for 7 to 10 days before performing the SAXS measurements.

Preparation of MMG samples hydrated in cell culture medium for SAXS analysis

The samples were prepared by using the thin-film method as described above with the following modification: the dry lipid films were hydrated with complete RPMI medium containing 10% (v/v) FBS by gentle vortexing immediately before performing the SAXS experiments. The final lipid concentration in the samples was kept constant (100 mg mL^{-1}).

SAXS measurements and data analysis

The X-ray measurements were performed at the beamline I911-4 (MAX II storage ring, MAX-lab synchrotron facility, Lund University, Sweden) at an operating electron energy of 1.5 GeV by using a 49-period, 3.5 T multipole wiggler producing a high-flux photon beam with a wavelength of 0.91 Å. The scattering patterns were recorded with a 2D image plate detector (165 mm MarCCD, MarResearch, Norderstedt, Germany). The camera was kept under vacuum during the data collection to minimize the background scattering. The samples were measured in custom-built sample holders and thermostated with a circulating water bath (Julabo, Seelbach, Germany). The two-dimensional scattering data were azimuthally averaged, normalized by the incident radiation intensity and the sample exposure time, and corrected for background and detector inhomogeneities by using the software BioXTAS RAW.[7] The radially averaged intensity I is given as a function of the scattering vector q ($q = 4 \sin \theta/\lambda$, where λ is the wavelength and 2θ is the scattering angle). The detector covered the q-range of interest from about 0.01 to 0.65 $Å^{-1}$. The synthetic analogue MMG-7 was measured at the beamline I711 (MAX II storage ring) at a wavelength of 1.201 Å and a slightly different q-range. Silver behenate [$H_3C(CH_2)_{20}COOAg$] with a d-spacing value of 58.38 Å was used as a standard to calibrate the angular scale.[8] The reflection laws for the L_α and the H_2 phases were applied to index the mesophases and calculate the corresponding unit lattice parameters.[9] The mean lattice parameters were deduced from the structure parameters calculated from each single reflection and presented with a sample standard deviation (SD).

Langmuir monolayers

Surfactant monolayers were formed at room temperature by spreading a total amount of 27.7 nmol MMG analogues dissolved in $CHCl_3$ onto an aqueous subphase consisting of 10 mM Tris buffer (pH = 7.4) in a KSV Minitrough 1 (KSV Instruments Ltd, Helsinki, Finland) with a surface area of 243 cm^2 by using a Hamilton microsyringe. The compression of the monolayers

was initiated 10 min after spreading the lipids to allow the organic solvent to evaporate. The monolayers were compressed with a barrier speed of 10 mm min^{-1}, and the surface pressure was measured by using a Wilhelmy platinum plate (KSV Instruments Ltd). Each sample ($n = 3$) was compressed once in three independent experiments ($n = 3$). The KSV software (KSV Instruments Ltd) was used for data analysis.

Statistics

Statistically significant differences were assessed by an analysis of variance (ANOVA) at a 0.05 significance level, followed by the Tukey's post-test. For the immunological data, differences were tested by two-way ANOVA followed by the Bonferroni post-test. Levels of statistical significance are indicated in the relevant figure legends.

3 Results and discussion

Synthesis of MMG analogues

A unique series of systematically varied novel MMG analogues (MMG-1 to MMG-7, Table 1) were prepared by using a modification[5] of a previously reported pathway.[4,10] The MMG analogues based on racemic synthetic corynomycolic acid analogues displaying an alternative (A) configuration consist of a 1 : 1 mixture of two diastereomers with (2*R*,3*S*,2′*R*) and (2*S*,3*R*,2′*R*) configurations (*i.e.* MMG-1, MMG-2, MMG-3 and MMG-4) or (2*R*,3*S*,2′*S*) and (2*S*,3*R*,2′*S*) configurations (MMG-5). The diastereomers could be distinguished by NMR due to minor differences in the chemical shifts of the signals corresponding to the atoms (both H and C) of the polar glycerol headgroups and of the adjacent part of the hydrophobic lipid acid moiety.[5] Similarly, the MMG analogues based on the native (N) racemic corynomycolic acid are mixtures of diastereomers with (2*R*,3*R*,2′*R*) and (2*S*,3*S*,2′*R*) configurations (MMG-6) or (2*R*,3*R*,2′*S*) and (2*S*,3*S*,2′*S*) configurations (MMG-7). Thus, both configurations of the headgroup (2′*R* and 2′*S*) were investigated. In addition, the length of the two hydrophobic alkyl chains was systematically varied and the series thus comprised MMG analogues with C_6/C_7 (MMG-4), C_{10}/C_{11} (MMG-3), C_{14}/C_{15} (MMG-1) and C_{16}/C_{17} alkyl chains (MMG-2).

The configuration of the lipid acid moiety affects the ability of the MMG analogues to activate human DCs *in vitro*

The degree of immunoactivation *in vitro* induced by the analogues was compared in primary cultures of immature monocyte-derived DCs generated from PBMCs from healthy human blood donors. It is preferable to use this type of cells because they are clinically more relevant than human or murine immune cell lines, despite a high donor-to-donor variation in their stimulatory sensitivity as a consequence of genetic polymorphisms in the human population. For cell stimulations, the MMG analogues were dissolved in isopropanol and coated onto tissue culture plates by gentle evaporation of the organic solvent. The cells were seeded in the coated tissue culture plates, and the production of the pro-inflammatory cytokine TNF-α was measured by ELISA after incubation at 37 °C for 22 hours to estimate the activation status of the cells.

The results show that the configuration of the lipid acid moiety of the MMG analogues affected their ability to activate human DCs (Fig. 2A). The TNF-α secretion was significantly increased from cells stimulated with the analogues having the alternative relative configuration of the lipid acid moieties (MMG-1 and MMG-5), as compared to the analogues with a native relative lipid acid moiety configuration (MMG-6 and MMG-7). By contrast, the glycerol headgroup configuration appeared not to influence the immunoactivating properties of the analogues, since no significant differences were observed between the 2′*R* and the 2′*S* configurations (MMG-1 as compared to MMG-5, and MMG-6 as compared to MMG-7). As expected, a high variation in the absolute TNF-α levels was observed between the donors (results not shown), and data were therefore normalized according to the maximal response of each individual donor.

The apparent inability of the analogues displaying a native relative lipid acid moiety configuration to activate the DCs led

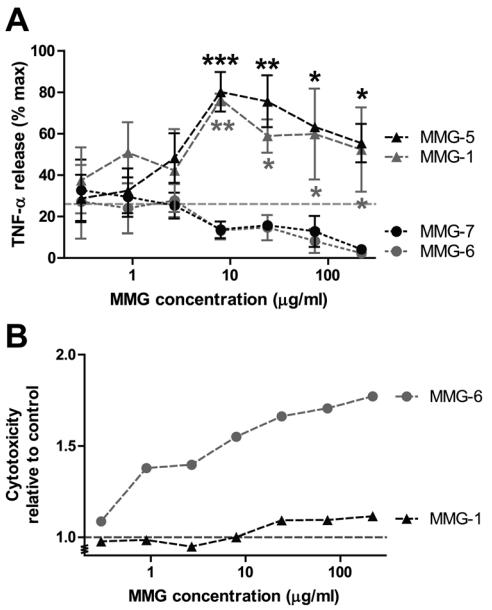

Fig. 2 The configuration of the lipid acid moiety is the major determinant for the degree of DC activation and influences cell viability *in vitro*. (A) Stimulation of human monocyte-derived DCs showed that MMG analogues with the alternative configuration of the lipid acid moiety [grey triangles (MMG-1): 2′*R*; black triangles (MMG-5): 2′*S*] exhibit higher stimulatory activities as compared to those of the corresponding MMG analogues with a native lipid acid moiety [grey circles (MMG-6): 2′*R*; black circles (MMG-7): 2′*S*], independently of the glycerol configuration. Symbols denote the relative mean TNF-α levels and error bars denote SEM ($n = 3$). The average background level of unstimulated cells is represented by the horizontal grey dashed line. Statistically significant differences between analogues differing in the lipid acid configuration, but not in the glycerol configuration, are indicated: *$p < 0.05$, **$p < 0.01$, and ***$p < 0.001$. (B) DCs from one representative donor were stimulated with MMG-1 and MMG-6 as above and the cytotoxicity was determined after 22 h by flow cytometry. Cytotoxicity is represented as the fold increase in the percentage of dead cells after MMG stimulation relative to the unstimulated control (indicated by the horizontal grey dashed line).

us to investigate if this stereochemistry was associated with an increase in cytotoxicity compared to the alternative configuration. Thus, we compared the cytotoxic effect of one of the analogues displaying a native relative configuration (MMG-6) with that of the corresponding analogue with the alternative relative configuration of the lipid acid moiety (MMG-1). The cells were stained with a cell viability dye after stimulation, and the percentage of dead cells was determined by flow cytometry. It was found that MMG-6 influenced the viability of the DCs to a much larger extent than MMG-1 at the highest concentrations tested (Fig. 2B), but even at the concentrations where the difference was minimal, MMG-6 was unable to activate the DCs (Fig. 2A). Thus, the optimal combination of high immunostimulatory potential and low cytotoxicity was achieved for the analogues displaying the alternative configuration of the lipid acid.

Human DC activation is highly dependent on the MMG alkyl chain length

Based on the results above, analogues with an alternative lipid acid configuration and displaying a 2′*R* glycerol ester moiety were chosen for further studies addressing the effect of the alkyl chain length of the MMG analogues on their ability to activate human DCs. For these studies, the proinflammatory cytokine panel measured was extended to include IL-6 and IL-8, and we consistently found that human DC activation was highly dependent on the lipid chain length: for the investigated concentration range, the MMG analogues with longer alkyl chains, *i.e.* C_{14}/C_{15} (MMG-1) and C_{16}/C_{17} (MMG-2), were able to significantly activate the cells, as evident by an enhanced production of all the investigated proinflammatory cytokines, as compared to the MMG analogues with shorter lipid chains (MMG-3 and MMG-4), which were less capable of stimulating the cells (Fig. 3). The lipids with relatively short alkyl chain lengths induced only cytokine production below the background level of unstimulated cells.

Since the low activity correlated with reduced viability for MMG-6, we hypothesized that MMG-3 and MMG-4 could also affect the viability of the cells *in vitro*. Therefore, the percentages of dead cells after stimulation with MMG-2, MMG-3 and MMG-4 were compared to the percentage of dead cells after stimulation with MMG-1. At the highest concentrations studied, the analogues with relatively short chain lengths were indeed much more toxic to the cells than analogues with longer chain length (Fig. 4). This correlated with the observation that the cytokine response was approaching that of unstimulated cells at the lowest concentrations of MMG-3 and MMG-4 but was lower than this background level at higher concentrations (Fig. 3). Thus, the C_{14}/C_{15} (MMG-1) and the C_{16}/C_{17} (MMG-2) analogues appear to be more immunoactivating, well-tolerated, and hence better suited as vaccine adjuvants for human use.

Other lipids tested for their potential as vaccine adjuvants in lipidic formulations also exhibit a clear chain length-dependent activity. Thus, it has recently been shown that longer lipid alkyl chains (C_{20}, C_{22} and C_{26}) of trehalose 6,6′-diesters (*e.g.* the dibehenate TDB, a synthetic analogue of mycobacterial cord factor) are required for the *in vitro* activation of mouse bone marrow-derived macrophages, whereas the shorter alkyl chain analogues (C_4, C_7, C_{10} and C_{16}) had no immunostimulatory effect.[11] In addition, optimal responses were obtained with the C_{22} analogue, which suggests an upper limit for the length of the lipid chain. However, the analogues were only tested at one concentration level, which may not be optimal for all the different analogues. Furthermore, the cytotoxic effect was not assessed, and it can therefore not be excluded that the absence of a response for the analogues with short lipid chains is an indirect result of cytotoxicity. We found that the MMG analogues that were least immunoactivating (MMG-3, MMG-4 and MMG-6) were also more toxic than the highly

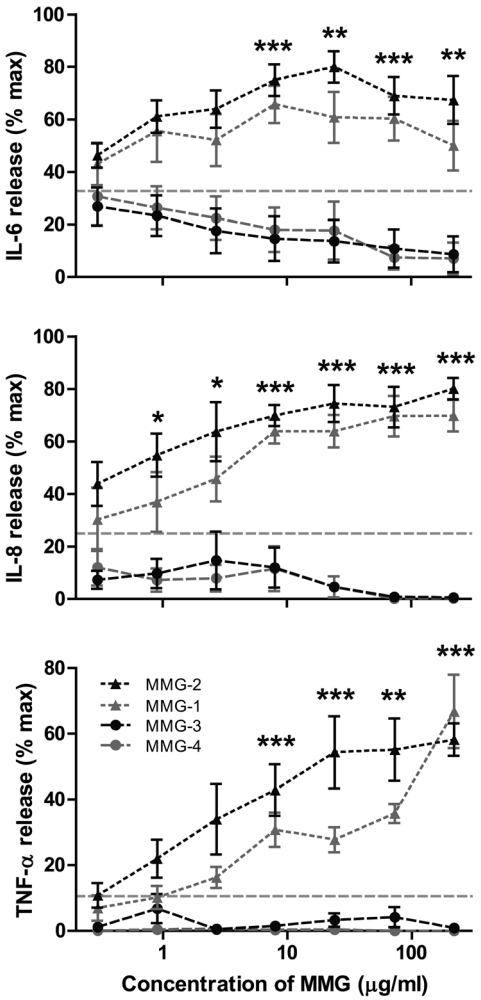

Fig. 3 The lipid chain length of MMG influences the immunostimulatory activity *in vitro*. Only MMG analogues with a lipid chain length of C_{14}/C_{15} (MMG-1, grey triangles) and C_{16}/C_{17} (MMG-2, black triangles) were able to induce the production of the pro-inflammatory cytokines IL-6 (top), IL-8 (middle) and TNF-α (bottom) in immature DCs derived from blood monocytes of healthy human blood donors, whereas the shorter analogues with a lipid chain length of C_{10}/C_{11} (MMG-3, black circles) and C_6/C_7 (MMG-4, grey circles) showed almost no activity. The results are normalized to the maximal response of each donor, and symbols denote the mean +/− SEM ($n = 4$–6). The average background levels are represented by the horizontal grey dashed lines. Statistically significant differences are indicated, where both MMG-1 and MMG-2 are statistically significant different from both MMG-3 and MMG-4: *$p < 0.05$, **$p < 0.01$, and ***$p < 0.001$.

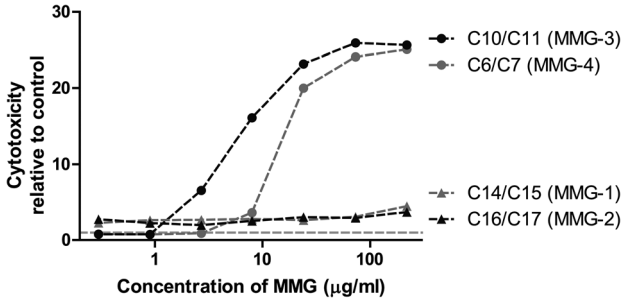

Fig. 4 MMG analogues with relatively short lipid chains (MMG-3 and MMG-4) exhibit increased cytotoxicity *in vitro*. The cytotoxic effect of MMG analogues with different lipid chain lengths was determined by stimulation of immature DCs derived from blood monocytes from a representative blood donor for 22 h and measuring the percentage of dead cells by flow cytometry. Cytotoxicity is represented as the fold increase in the percentage of dead cells after MMG stimulation compared to unstimulated control cells.

immunoactivating analogues (MMG-1 and MMG-2) which could suggest a behavioral resemblance between these structures. For another type of lipid adjuvant, LPS, the immunoactivating property *in vitro* has been shown to be highly dependent on the size and conformation of the apolar region and closely related to their nanostructure in that system.[12,13]

The nature of the interaction between MMGs and the components of the plasma membrane is currently unknown, but the involvement of a receptor-specific recognition is implied *via* the activation of downstream cellular signaling pathways and proinflammatory cellular responses. Although MMG is not a glycolipid, it is relevant to note that certain glycolipids (*e.g.* mycobacterial cord factor) exhibit immunoactivating characteristics similar, but not identical, to MMG.[10] These glycolipids have been shown to bind to the CLR Mincle and signal through the Syk-Card9 pathway leading to upregulation of granulocyte-colony stimulating factor and IL-6[2] as well as secretion of TNF-α and IL-6 by murine macrophages.[3] In addition, lysophospholipids have been reported to induce IL-8 and IL-6 secretion from immature DCs apparently *via* a G-protein-coupled receptor signaling through ERK2.[14]

DC-activating MMG analogues adopt L_α structures, whereas MMG analogues that exhibit modest activity form H_2 structures

Since the *in vitro* findings suggested that the nanostructural characteristics of the MMG analogues might influence their ability to activate DCs, SAXS experiments were performed to improve the understanding of the nanostructural characteristics of the self-assembled phases formed by the surfactant-like MMG analogues upon exposure to excess buffer or to a biologically relevant medium. Although the lipid concentrations were different in the two studies due to differing experimental requirements, *i.e.* a low lipid concentration in the *in vitro* study due to toxicity issues and a high lipid concentration in the SAXS study due to a high signal-to-noise-ratio, the lipids studied were under fully hydrated conditions in both studies. As the fully hydrated self-assembled structure is independent of the lipid concentration, the structures revealed by the SAXS study can be directly related to the structures presented to the cells *in vitro*.

The fully hydrated MMG analogues displayed a rich polymorphism (Fig. 5) including the formation of lyotropic lamellar and non-lamellar liquid crystalline phases [*i.e.* lamellar (L_α) and inverse hexagonal (H_2) structure, respectively]. The present study demonstrates that analogues differing in the lipid acid stereochemistry may reveal pronounced differences in their

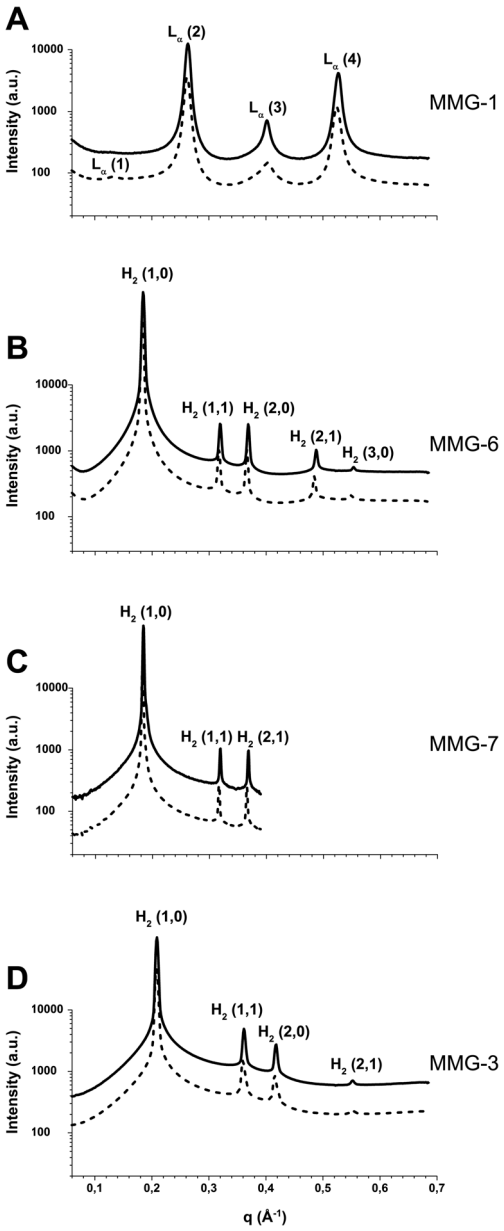

Fig. 5 SAXS diffraction patterns for fully hydrated MMG analogues at 35 °C (dashed line) and 40 °C (solid line). The *q*-ranges on the *x*-axes of all four graphs are equal to facilitate comparisons of peak positions. (A) The fully hydrated MMG-1 analogue. Four reflections corresponding to a neat lamellar (L_α) phase are evident. (B) The fully hydrated MMG-6 analogue. The observed five peaks are compatible with the first characteristic reflections of an inverse hexagonal (H_2) phase. (C) The fully hydrated MMG-7 analogue (a neat H_2 phase). This analogue was measured at a different beamline and *q*-range. (D) The fully hydrated MMG-3 analogue (a neat H_2 phase).

behavior at the molecular level upon exposure to excess water. A similar observation was made recently by Jacquemet *et al.*, who report that the stereochemistry of the central cyclopentane unit of two synthetic archaeal bipolar lipid analogues has a remarkable effect on their self-assembled nanostructures.[15]

To exemplify the drastic impact of the lipid acid stereochemistry of MMG on the fully hydrated nanostructures, Fig. 5 (panels A and B) shows the SAXS diffraction patterns for the fully hydrated MMG-1 and MMG-6 at biologically relevant temperatures of 35 °C and 40 °C. The obtained SAXS data for the fully hydrated MMG-1 analogue indicates the formation of a neat lamellar (L_α) phase at the investigated temperatures. At 35 °C, the SAXS pattern shows four characteristic peaks of the L_α phase, and the calculated lattice spacing for this phase is approximately 48 Å (Table 2). A significant structural change was observed upon varying the configuration of the lipid acid moiety, as it was found that the analogue with the native configuration (MMG-6) displayed a neat inverse hexagonal (H_2) phase in excess buffer within the investigated temperature range (Fig. 5B). The observed peaks were compatible with the (1,0), (1,1), (2,0), (2,1) and (3,0) reflections characteristic for an H_2 phase. The unit cell parameter of this phase, which corresponds to the distance between adjacent hydrophilic cylindrical nanochannels embedded in a two-dimensional hydrophobic continuous matrix, was calculated to be approximately 39.6 Å at 35 °C.

The remarkable influence of the lipid acid configuration on the structural characteristics of the investigated fully hydrated lipid systems is most likely linked to variations in the overall lipid molecular geometry, which dictates the self-assembling properties. MMG-1 has a mean molecular area (A) of approximately 35.3 $Å^2$,[5] which is close to the value of 40.0 $Å^2$ derived from pressure *versus* area isotherms for closely packed double alkyl chains.[16] Thus MMG-1 presumably adopts a rod-like molecular structure, and it is therefore characterized by its tendency to form planar bilayers upon exposure to excess buffer. The propensity of the fully hydrated MMG-6 to form a non-lamellar H_2 phase may be explained by the different spatial orientation of the alkyl chains induced by the altered stereochemistry in the lipid acid moiety that affects the overall molecular shape. It is plausible that the hydrophobic alkyl tails of this double-chained lipid are not closely packed in the liquid crystalline phase but rather adopt a wedge-shaped molecular structure that results in the formation of a non-lamellar phase. The drastic impact of the amphiphilic molecular shape of natural and synthetic surfactant-like lipids on the self-assembling properties upon exposure to water is well-known and has been demonstrated in various studies.[17–19]

The study of MMG analogues differing in the stereochemistry of the glycerol moiety but with similar length of the hydrophobic tails revealed no significant difference in the self-assembled structures. As an example, Fig. 5B and C show the SAXS scattering patterns obtained for the fully hydrated MMG-6 and MMG-7. Clearly for both fully hydrated analogues, the observed peaks in their SAXS scattering patterns are virtually identical and indicate the formation of a neat H_2 nanostructure. Similar SAXS investigations were performed on other analogues including MMG-5, and the obtained data showed no significant effect of changing the glycerol stereochemistry (the structural parameters for MMG-5 are presented in Table 2). These results suggest that variation in the polar headgroup configuration does not significantly affect the water-headgroup (the hydration level) or the headgroup–headgroup interactions in excess water, and therefore very similar structures are obtained. These results are different from previous investigations on the influence of headgroup configuration on synthetic glycolipid–water binary systems.[16] In these cases it was found that the stereochemistry of the oligosaccharide headgroups affects the structural properties of the fully hydrated glycolipids. In addition, the properties of different glycolipids are influenced by the nature of the anomeric linkage (*i.e.* α- *versus* β-anomers) as well as by the chirality of the asymmetrical glycerol moieties.[20–22]

Various reports show that the hydration-induced nanostructures of self-assembled systems upon exposure to excess water are modulated by the contribution of both the polar headgroup and the hydrophobic tails (the lipid molecular structure).[17,19–21,23–26] We therefore investigated whether the observed link between DC activation and lamellar phase formation would also apply to the MMG analogues with shorter alkyl chains, which were poor activators of DCs, and in addition were more toxic to the cells. Hence, SAXS experiments were performed to characterize the nanostructure of the fully hydrated MMG-3 system displaying shorter alkyl chains of C_{10}/C_{11}. The obtained SAXS data at 35 °C indicate that the fully hydrated structure is a neat inverse hexagonal (H_2) phase (Fig. 5D). The lattice parameter of the hexagonal phase was calculated to be approximately 35 Å (Table 2). As discussed above, double-chained surfactant-like lipids, displaying relatively long alkyl chains, may adopt a rod-like molecular shape due to the tightly packed tails favored by strong hydrophobic interactions. Therefore, they tend to form lamellar phases in excess buffer, whereas lipids with shorter alkyl chains such as MMG-3, most likely adopt a wedge-shaped amphiphilic molecular structure (resulting in less densely packed alkyl chains), although their mean molecular area is close to 40 Å. This explains the tendency of the fully hydrated MMG-3 system to form the non-lamellar phase H_2. The SAXS characterization of

Table 2 Structure parameters for the lamellar (L_α) and the inverse hexagonal (H_2) phases derived from SAXS investigations of fully hydrated MMG analogue-based systems

Analogue	Temperature (°C)	Phase	Mean $a \pm$ SD (Å)	
MMG-1	35	L_α	47.7 ± 0.6	($n = 4$)
	40	L_α	47.4 ± 0.5	
MMG-3	35	H_2	34.95 ± 0.09	($n = 4$)
	40	H_2	34.76 ± 0.01	
MMG-5	35	L_α	47.6 ± 0.7	($n = 3$)
	40	L_α	47.5 ± 0.5	
MMG-6	35	H_2	39.62 ± 0.02	($n = 5$)
	40	H_2	39.35 ± 0.02	
MMG-7	35	H_2	39.68 ± 0.02	($n = 3$)
	40	H_2	39.40 ± 0.01	

the fully hydrated MMG-4 analogue was excluded from the present investigation due to the low-viscous oily nature of this system at room temperature, but it is most likely prone to form a micellar solution coexisting with excess buffer. The fully hydrated MMG-2 exhibited a temperature-dependent complex behavior (results not shown), and further studies are therefore essential for ensuring a complete characterization of its self-assembled nanostructure.

To enable a direct comparison of the SAXS study to the *in vitro* studies, a SAXS study was also performed on the MMG analogues hydrated in cell culture medium containing 10% (v/v) serum. The obtained data showed no detectable effect of changing the aqueous buffer to serum-containing medium (results not shown). This implies that the presence of other solutes and serum proteins in the cell culture medium under the applied experimental conditions has no significant impact on the self-assembled nanostructures. Thus the nanostructures characterized by SAXS are most likely directly comparable to the nanostructures present in the *in vitro* immunological studies.

The lipid chain length and stereochemistry affect the packing of MMG monolayers at the air–water interface

The Langmuir technique was employed to understand the effect of the stereochemistry of the polar headgroup and the lipid acid moiety, as well as the influence of alkyl chain length on the spatial orientation of the alkyl chains, the overall molecular shape, and the packing ability of the MMG analogues. Although the lipid monolayer is not directly comparable to the three-dimensional structures present in the *in vitro* and the SAXS studies, the Langmuir technique can be utilized to acquire a more in-depth understanding of the interactions at the molecular level. Furthermore, SAXS measurements at 25 °C on the analogues MMG-1, MMG-3, MMG-5, MMG-6 and MMG-7 revealed that the structure of these analogues is unchanged between 25 °C and 40 °C and can thus be directly related to the Langmuir observations.

Langmuir monolayers of MMG analogues at the air–water interface were compressed while monitoring the surface pressure by using a Wilhelmy plate (Fig. 6). The values for the surface pressure (Π) and the mean molecular area (A) at the monolayer collapse and at the phase transition from the liquid-expanded to the liquid-condensed phase are listed in Table 3. The phase transitions and the collapse points were estimated from the compression modulus (C_S^{-1}) *versus* Π dependency, where C_S^{-1} is defined as:[27]

$$C_S^{-1} = -A\frac{d\Pi}{dA}.$$

A characteristic minimum for the C_S^{-1} *versus* Π dependency for the monolayer reflects the phase transition from the liquid-expanded to the liquid-condensed states of the monolayer, whereas the surface pressure at $(d\Pi/dA) = 0$ identifies the monolayer collapse.

Monolayers of MMG-1 showed a phase transition from the liquid-expanded state to the liquid-condensed state at a surface pressure of 14.7 mN m^{-1} with a mean molecular area of 61.4 Å^2, and they collapsed at a surface pressure of 53.4 mN m^{-1} with a mean molecular area of 35.3 Å^2 (Fig. 6 and Table 3) as reported previously.[5]

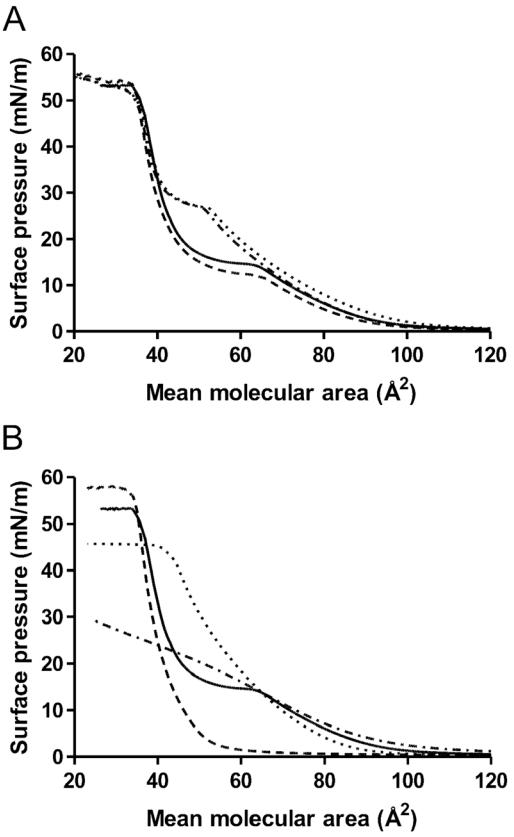

Fig. 6 Pressure/area isotherms of Langmuir monolayers of MMG analogues on Tris buffer subphases. The total lipid concentrations of the different monolayers are identical in all experiments. The curves represent averages of three experiments. (A): Effect of stereochemistry of the lipid acid moiety and the glycerol headgroup. MMG-1 (solid), MMG-5 (dash), MMG-6 (dot), MMG-7 (dash-dot). (B): Effect of chain length. MMG-1 (solid), MMG-2 (dash), MMG-3 (dot), MMG-4 (dash-dot).

Lipid monolayers consisting of MMG analogues differing in the stereochemistry of the lipid acid moiety as well as in the glycerol headgroup were compared (Fig. 6A). The stereochemistry around the hydrocarbon chains (native *versus* alternative configuration) accounted for the pronounced differences seen between the Π–A isotherms of the monolayers of MMG-1 and MMG-5 (alternative configuration) and the Π–A isotherms of the analogues with a native configuration (MMG-6 and MMG-7, Fig. 6A). In particular, the mean molecular area of the MMG analogues at the liquid-expanded to liquid-condensed phase transition was affected by the lipid acid stereochemistry (Table 3): a statistically significant decrease in the mean molecular area was observed at the liquid-expanded to liquid-condensed phase transition from about 61–64 Å^2 for analogues with the alternative configuration (MMG-1 and MMG-5) to about 50–52 Å^2 for analogues with the native configuration (MMG-6 and MMG-7). In addition, the surface pressure was significantly increased at the phase transition from about

Table 3 Surface pressures (Π) and mean molecular areas (A) at the phase transition and at the collapse point for Langmuir monolayers of MMG analogues[a]

MMG analogue	Collapse point Π (mN m^{-1})	A (Å^2)	Phase transition Π (mN m^{-1})	A (Å^2)
MMG-1	53.4 ± 0.5	35.3 ± 1.3	14.7 ± 0.4	61.4 ± 1.7
MMG-2	57.7 ± 0.2***	31.4 ± 0.5*	[b]	[b]
MMG-3	45.5 ± 0.2***	39.2 ± 1.9*	[b]	[b]
MMG-4	[b]	[b]	[b]	[b]
MMG-5	54.5 ± 1.4	33.5 ± 1.3	12.3 ± 0.3***	64.2 ± 2.1
MMG-6	52.7 ± 0.4	31.6 ± 0.4*	26.8 ± 0.2***	51.9 ± 0.1***
MMG-7	53.1 ± 0.5	30.2 ± 0.3**	27.0 ± 0.2***	50.3 ± 0.9***

[a] Results denote mean ± SD ($n = 3$). Results significantly different from MMG-1 are indicated: *$p < 0.05$, **$p < 0.01$ and ***$p < 0.001$. [b] No detectable phase transition or collapse point.

12–15 mN m^{-1} for the analogues with the alternative configuration (MMG-1 and MMG-5) to about 27 mN m^{-1} for the analogues with the native configuration (MMG-6 and MMG-7). These findings are in accordance with other studies indicating that the stereochemistry of glycolipids affects both the surface pressure and the packing of lipid monolayers, especially around the phase transition.[28,29] Most likely, this difference in the monolayer behavior is due to altered interactions between the lipid alkyl chains resulting in differences in the molecular packing of the films. Thus, there seems to be a contracting effect around the phase transition in monolayers of MMG analogues with an alternative configuration as compared to monolayers of analogues with a native configuration. This may be explained by more favorable hydrophobic interactions between the hydrocarbon chains of analogues with an alternative configuration resulting in an overall rod-like molecular structure, as opposed to the putatively wedge-shaped molecular structure of the analogues with a native configuration, for which a higher surface pressure is needed to compress the monolayer from a liquid-expanded to a liquid-condensed phase. This result correlates well with the observations that the native analogues form non-lamellar H_2 phases in excess buffer, whereas analogues with the alternative configuration self-assemble into lamellar structures, which may more effectively interact with the APCs.

The stereochemistry did not significantly affect the surface pressure at the collapse point, which suggests that the interaction between the glycerol headgroups and the water subphase does not depend on the stereochemistry of the glycerol moiety. However, it is important to mention that the mean molecular area was slightly, albeit statistically significant, decreased for analogues with a native lipid acid configuration (MMG-6 and MMG-7) as compared to those with an alternative configuration (MMG-1 and MMG-5), as discussed in the previous section. This shows that the spatial orientation of the lipid tails influences the mean molecular area and the packing parameter, as also demonstrated by the significant effect of the lipid acid stereochemistry on the structural characteristics of these surfactant-like lipids under fully hydrated conditions (*i.e.* the SAXS investigations). In contrast, the stereochemistry of the glycerol headgroup did not affect the mechanical properties of the MMG monolayers at the air–water interface since the isotherms were similar for MMG-1 and MMG-5, as well as for MMG-6 and MMG-7 (Fig. 6A and Table 3).

A clear correlation was furthermore observed between the lipid chain length and the appearance of the resulting isotherms: for the longer chain length analogue MMG-2 and the shorter analogues MMG-3 and MMG-4, no phase changes were observed (Fig. 6B). The presence of a phase transition has also previously been demonstrated to be dependent on the length of the lipid alkyl chains.[29] In addition, the surface pressure as well as the mean molecular area at the collapse point in the present study was affected by the chain length. Increasing the chain length resulted in a significantly decreased mean molecular area as well as a significantly increased surface pressure at the collapse point (*cf.* the comparison of the behavior of MMG-2 and MMG-3, Fig. 6B and Table 3). This suggests that monolayers of lipids with longer alkyl chains are able to pack more densely than monolayers of lipids with shorter alkyl chains, which most likely is the result of stronger van der Waals attractive forces between longer alkyl chains. A comparison of two phospholipids with chain lengths of 18 or 16 carbon atoms, respectively, also suggested a more dense packing of the lipid molecules with the longest alkyl chains.[30] For the shortest analogue (MMG-4), in addition to the lack of a phase transition, no monolayer collapse was observed (Fig. 6B), which suggests that this analogue is not able to form a stable monolayer at the air–water interface due to its short alkyl chains, but rather exists in the buffer subphase as most likely an inverted type micellar (L_2) phase. Again there is a neat correlation with the observations from the SAXS studies suggesting that longer alkyl chain lengths form lamellar lipid structures, whereas analogues of shorter alkyl chain lengths self-assemble into non-lamellar H_2 structures, resulting in reduced immunostimulation.

Our findings demonstrate that the interpretation of the *in vitro* evaluations of lipid or amphiphilic adjuvant compounds may be drastically influenced by variations in their biophysical properties, which can lead to the formation of nanostructures that do not present the receptor-interacting part to the APCs or which increases the cytotoxicity. Thus, our data indicate that there is a risk of getting false-negative results in these types of assays because the effect of the immunopotentiator is not only

dependent on the structure of the molecular compound, which is decisive for the receptor binding, but also on its colligative properties, which are reflected by the supramolecular structure.

4 Conclusions

Our experimental findings suggest that the stereochemistry of the lipid acid moiety as well as the length of the hydrophobic alkyl chains determine the immunostimulating properties of the MMG analogues *in vitro*. The highest activation level was observed for the MMG analogues with an alternative configuration of the lipid acid moiety (corynomycolic acid) displaying relatively long hydrophobic alkyl chains (C_{14}/C_{15} and C_{16}/C_{17}). A favorable balance between immune response and cytotoxicity was obtained upon exposure to MMG analogues forming self-assembled nanostructures adopting the lamellar phase, whereas MMG analogues forming the inverted hexagonal phase activated DCs to a lower extend and were also more cytotoxic. Although further studies are required to elucidate whether the observed differences in the immunostimulating properties of the MMG analogues are related to differences in the affinity to a putative cell-associated receptor, it is clear that they correlate with differences in the supramolecular characteristics of the self-assembled nanostructures. We have thus demonstrated, that an interdisciplinary approach of combining structural analysis with immunological characterisation is important. Our findings suggest that the biophysical properties should be considered when evaluating novel lipid adjuvants *in vitro* in order to avoid drawing conclusions based on false-negative results.

Conflicts of interest

Else Marie Agger and Peter Andersen are co-inventors on a patent covering MMG for use in adjuvant formulations.

Acknowledgements

Thanks to K. Vissing, L. Bentzen, E. Pedersen, T. Khilji, M. Nielsen (University of Copenhagen), R. F. Jensen, J. F. Buhelt, V. Skov and L. El-Haj (Statens Serum Institut), T. Plivelic and A. Labrador (MAX-lab, Lund, Sweden) for excellent technical assistance. This work was funded by the Danish National Advanced Technology Foundation, the Drug Research Academy, Statens Serum Institut and the European Commission (contract no. LSHP-CT-2003-503367 and FP7-HEALTH-F3-2009-241745). We acknowledge the Danish Agency for Science, Technology and Innovation for the Zetasizer Nano ZS and the Drug Research Academy for co-funding the KSV Minithrough 1. Max-lab is acknowledged for providing beamtime and the instrument for the SAXS studies. The research leading to the SAXS results has received funding from the European Community's Seventh Framework Programme (FP7/2007–2013) under grant agreement no. 226716.

References

1 D. A. Johnson, D. S. Keegan, C. G. Sowell, M. T. Livesay, C. L. Johnson, L. M. Taubner, A. Harris, K. R. Myers, J. D. Thompson, G. L. Gustafson, M. J. Rhodes, J. T. Ulrich, J. R. Ward, Y. M. Yorgensen, J. L. Cantrell and V. G. Brookshire, *J. Med. Chem.*, 1999, **42**, 4640–4649.
2 H. Schoenen, B. Bodendorfer, K. Hitchens, S. Manzanero, K. Werninghaus, F. Nimmerjahn, E. Marie, S. Stenger, P. Andersen, J. Ruland, G. D. Brown, C. Wells and R. Lang, *J. Immunol.*, 2010, **184**, 2756–2760.
3 E. Ishikawa, T. Ishikawa, Y. S. Morita, K. Toyonaga, H. Yamada, O. Takeuchi, T. Kinoshita, S. Akira, Y. Yoshikai and S. Yamasaki, *J. Exp. Med.*, 2009, **206**, 2879–2888.
4 C. S. A. Andersen, I. Rosenkrands, A. W. Olsen, P. Nordly, D. Christensen, R. Lang, C. Kirschning, J. M. Gomes, V. Bhowruth, D. E. Minnikin, G. S. Besra, F. Follmann, P. Andersen and E. M. M. Agger, *J. Immunol.*, 2009, **183**, 2294–2302.
5 P. Nordly, K. S. Korsholm, E. A. Pedersen, T. S. Khilji, H. Franzyk, L. Jorgensen, H. M. Nielsen, E. M. Agger and C. Foged, *Eur. J. Pharm. Biopharm.*, 2011, **77**, 89–98.
6 V. Bhowruth, D. E. Minnikin, E. M. M. Agger, P. Andersen, V. W. Bramwell, Y. Perrie and G. S. Besra, *Bioorg. Med. Chem. Lett.*, 2009, **19**, 2029–2032.
7 S. S. Nielsen, K. N. Toft, D. Snakenborg, M. G. Jeppesen, J. K. Jacobsen, B. Vestergaard, J. P. Kuttera and L. Arleth, *J. Appl. Crystallogr.*, 2009, **42**, 959–964.
8 T. C. Huang, H. Toraya, T. N. Blanton and Y. Wu, *J. Appl. Crystallogr.*, 1993, **26**, 180–184.
9 M. Rappolt, in *The Biologically Relevant Lipid Mesophases as "Seen" by X-Rays*, Elsevier, 2006, ch. 9, vol. 5, pp. 253–283.
10 C. S. Andersen, E. M. M. Agger, I. Rosenkrands, J. M. Gomes, V. Bhowruth, K. J. Gibson, R. V. Petersen, D. E. Minnikin, G. S. Besra and P. Andersen, *J. Immunol.*, 2009, **182**, 424–432.
11 A. A. Khan, S. H. Chee, R. J. McLaughlin, J. L. Harper, F. Kamena, M. S. M. Timmer and B. L. Stocker, *ChemBioChem*, 2011, **12**, 2572–2576.
12 A. B. Schromm, K. Brandenburg, H. Loppnow, U. Zähringer, E. T. Rietschel, S. F. Carroll, M. H. Koch, S. Kusumoto and U. Seydel, *J. Immunol.*, 1998, **161**, 5464–5471.
13 K. Brandenburg, H. Mayer, M. H. Koch, J. Weckesser, E. T. Rietschel and U. Seydel, *Eur. J. Biochem.*, 1993, **218**, 555–563.
14 D. Öz Arslan, W. Rüscher, D. Myrtek, M. Ziemer, Y. Jin, B. B. Damaj, S. Sorichter, M. Idzko, J. Norgauer and A. A. Maghazachi, *J. Leukocyte Biol.*, 2006, **80**, 287–297.
15 A. Jacquemet, C. Mériadec, L. Lemiègre, F. Artzner and T. Benvegnu, *Langmuir*, 2012, **28**, 7591–7597.
16 M. Hato, H. Minamikawa, K. Tamada, T. Baba and Y. Tanabe, *Adv. Colloid Interface Sci.*, 1999, **80**, 233–270.
17 C. Fong, T. Le and C. J. Drummond, *Chem. Soc. Rev.*, 2012, **41**, 1297–1322.
18 A. Yaghmur, B. Sartori and M. Rappolt, *Langmuir*, 2012, **28**, 10105–10119.
19 S. Hyde, Z. Blum, T. Landh, S. Lidin, B. W. Ninham, S. Andersson and K. Larsson, *The Language of Shape: The Role of Curvature in Condensed Matter: Physics, Chemistry and Biology*, Elsevier Science B.V., 1st edn, 1996.
20 A. Sen, S. W. Hui, D. A. Mannock, R. N. Lewis and R. N. McElhaney, *Biochemistry*, 1990, **29**, 7799–7804.

21 J. M. Seddon, N. Zeb, R. H. Templer, R. N. McElhaney and D. A. Mannock, *Langmuir*, 1996, **12**, 5250–5253.
22 D. A. Mannock, R. N. A. H. Lewis and R. N. McElhaney, *Chem. Phys. Lipids*, 1990, **55**, 309–321.
23 P. M. Duesing, J. M. Seddon, R. H. Templer and D. A. Mannock, *Langmuir*, 1997, **13**, 2655–2664.
24 A. Yaghmur, P. Laggner, M. Almgren and M. Rappolt, *PLoS One*, 2008, **3**(11), e3747, DOI: 10.1371/journal.pone.0003747.
25 J. Howe, M. von Minden, T. Gutsmann, M. H. Koch, M. Wulf, S. Gerber, G. Milkereit, V. Vill and K. Brandenburg, *Chem. Phys. Lipids*, 2007, **149**, 52–58.
26 A. Yaghmur, L. Paasonen, M. Yliperttula, A. Urtti and M. Rappolt, *J. Phys. Chem. Lett.*, 2010, **1**, 962–966.
27 D. Vollhardt and V. B. Fainerman, *Adv. Colloid Interface Sci.*, 2006, **127**, 83–97.
28 K. Matsumoto, H. Sakai, K. Ohta, H. Kameda, F. Sugawara, M. Abe and K. Sakaguchi, *Chem. Phys. Lipids*, 2005, **133**, 203–214.
29 E. Durand, M. Welby, G. Laneelle and J. F. Tocanne, *Eur. J. Biochem.*, 1979, **93**, 103–112.
30 P. Wydro and K. Witkowska, *Colloids Surf., B: Biointerfaces*, 2009, **72**, 32–39.